

4H Leukodystrophy: A Brain Magnetic Resonance Imaging Scoring System

Suzanne Vrij-van den Bos^{1,*} Janna A. Hol^{1,*} Roberta La Piana^{2,3,*} Inga Harting⁴ Adeline Vanderver⁵
 Frederik Barkhof^{6,7} Ferdy Cayami^{1,8} Wessel N. van Wieringen⁹ Petra J. W. Pouwels^{10,11}
 Marjo S. van der Knaap^{1,11,12} Geneviève Bernard^{3,13,14,‡} Nicole I. Wolf^{1,11,‡}

¹ Department of Child Neurology, VU University Medical Center, Amsterdam, The Netherlands

² Laboratory of Neurogenetics of Motion and Department of Neuroradiology, Montreal Neurological Institute and Hospital, McGill University, Montreal, Canada

³ Department of Neurology and Neurosurgery, and Pediatrics, McGill University, Montreal, Canada

⁴ Department of Neuroradiology, University Hospital Heidelberg, Heidelberg, Germany

⁵ Department of Neurology, Children's National Medical Center, Washington DC and George Washington University School of Medicine, Washington, Dist. of Columbia, United States

⁶ Department of Radiology, VU University Medical Center, Amsterdam, The Netherlands

⁷ Institute of Neurology and Health Care Engineering, University College London, London, United Kingdom

⁸ Department of Clinical Genetics, VU University Medical Center, Amsterdam, The Netherlands

⁹ Department of Clinical Epidemiology and Biostatistics, VU University Medical Center and Department of Mathematics, VU University, Amsterdam, The Netherlands,

¹⁰ Department of Physics and Medical Technology, VU University Medical Center, Amsterdam, The Netherlands,

¹¹ Amsterdam Neuroscience, Amsterdam, The Netherlands,

¹² Department of Functional Genomics, VU University, Amsterdam, The Netherlands,

¹³ Department of Medical Genetics, McGill University Health Center, Montreal Children's Hospital, Montreal, Canada,

¹⁴ Child Health and Human Development Program, Research Institute of the McGill University Health Center, Montreal, Canada

Address for correspondence Nicole I. Wolf, MD, PhD, Department of Child Neurology, VU University Medical Center, Postbox 7057, 1007 MB, Amsterdam, The Netherlands (e-mail: n.wolf@vumc.nl).

Neuropediatrics 2017;48:152–160.

Abstract

Keywords

- ▶ 4H
- ▶ leukodystrophy
- ▶ MRI
- ▶ hypomyelination

4H (hypomyelination, hypodontia and hypogonadotropic hypogonadism) leukodystrophy (4H) is an autosomal recessive hypomyelinating white matter (WM) disorder with neurologic, dental, and endocrine abnormalities. The aim of this study was to develop and validate a magnetic resonance imaging (MRI) scoring system for 4H. A scoring system (0–54) was developed to quantify hypomyelination and atrophy of different brain regions. Pons diameter and bicaudate ratio were included as measures of cerebral and brainstem atrophy, and reference values were determined using

* The authors contributed equally to this work.

‡ The authors contributed equally to this work.

controls. Five independent raters completed the scoring system in 40 brain MRI scans collected from 36 patients with genetically proven 4H. Interrater reliability (IRR) and correlations between MRI scores, age, gross motor function, gender, and mutated gene were assessed. IRR for total MRI severity was found to be excellent (intraclass correlation coefficient: 0.87; 95% confidence interval: 0.80–0.92) but varied between different items with some (e.g., myelination of the cerebellar WM) showing poor IRR. Atrophy increased with age in contrast to hypomyelination scores. MRI scores (global, hypomyelination, and atrophy scores) significantly correlated with clinical handicap ($p < 0.01$ for all three items) and differed between the different genotypes. Our 4H MRI scoring system reliably quantifies hypomyelination and atrophy in patients with 4H, and MRI scores reflect clinical disease severity.

Introduction

Hypomyelinating disorders constitute a heterogeneous group of different disease entities, defined by a permanent and significant lack of central nervous system myelin.¹ One of the striking features of these conditions is the large variation in severity: some patients have virtually no neurologic signs and normal cognition, and others are severely affected early on and wheelchair-bound, usually with less profoundly affected cognitive function. A recent study aimed at correlating gross motor function (GMF) with quantitative white matter (WM) magnetic resonance imaging (MRI) parameters and showed that in a heterogeneous group of patients with hypomyelination, it is mainly the lack of myelin that code-termines motor handicap.²

Short of quantitative information, it is desirable to grade imaging severity tailored to a single hypomyelinating entity by assessing the degree of myelin deficit and atrophy using conventional T1- and T2-weighted images and to correlate these scores with GMF. This would be helpful for retrospective studies, as these images are available for most patients, as well as for routine clinical use, providing useful information for future therapeutic trials. Such scoring systems have proven to be a valuable tool for other leukodystrophies such as X-linked adrenoleukodystrophy (X-ALD) and metachromatic leukodystrophy (MLD).^{3,4} Recently, a scoring system for Pelizaeus–Merzbacher’s disease (PMD), the most common hypomyelinating disorder, was published but was not available when we were embarking on this project.⁵

We aimed to develop a scoring system for a hypomyelinating disorder, 4H leukodystrophy (4H), the second most common hypomyelinating entity⁶ characterized by hypomyelination, hypodontia, and hypogonadotropic hypogonadism.^{7–9} Recessive mutations in either *POLR3A*, *POLR3B* or *POLR1C*, encoding subunits of RNA polymerase III and I, cause almost all cases with the clinical diagnosis of 4H, with mutations in *POLR3B* explaining the majority of cases in Central and Western Europe and mutations in *POLR1C* being the least frequent.^{10–14} Clinical variation is wide, ranging from mild, even subclinical ataxia, to severe motor handicap, and the course is, after a stable phase ranging from 2 to 3 years to more than 10 years, slowly progressive in most. In addition to hypomyelination, MRI findings

comprise early cerebellar atrophy, especially in cases with mutations in *POLR3B*, and late, milder supratentorial brain atrophy including thinning of the corpus callosum.¹⁵ Some WM structures are better myelinated: the optic radiation, the ventrolateral thalamus, the pyramidal tract in the posterior limb of the internal capsule, the dentate nucleus, and the medial lemniscus in the brain stem.¹⁶ We present a novel MRI rating scale that reflects these findings and determined its interrater reliability (IRR) and clinical validity.

Patients and Methods

Patient Selection

Brain MRI scans were retrospectively collected from patients with genetically proven 4H from the databases of VU Medical Center in Amsterdam, the Netherlands, and Montreal Children’s Hospital in Montreal, Canada. Scans had been performed at different scanners (1.5 and 3T) following different protocols at different centers and were included when at least axial T2- and T1-weighted images and a sagittal series were available. Only patients with MRI scans acquired at 24 months of age or later were included because normal myelination is not completed before this age.

Controls

A total of 86 healthy individuals (45 males, 41 females) with a median age of 6.5 years (range: 0–29) served as a control group. We focused on younger ages as there were no good normal values for bicaudate ratio (BCR) and brainstem diameter available in contrast to adults. Reasons for MRI were headache, mild epilepsy without focal neurologic abnormalities, or mild developmental delay. All were evaluated by (pediatric) neurologists and radiologists, and no abnormal neurologic or MRI findings were identified.

Magnetic Resonance Imaging Scoring

We developed a scoring system to assess hypomyelination and atrophy of different brain regions (→ **Table 1**). Hypomyelination was graded separately on axial T1- and T2-weighted images, depending on the signal intensity in relation to the caudate nucleus. Atrophy was visually scored for selected structures (cerebellum, corpus callosum; → **Fig. 1**) and

Table 1 Brain MRI scoring system for 4H leukodystrophy

Hypomyelination score	T1W	T2W	T1W + T2W
Frontal white matter			
Subcortical	0–2	0–2	0–4
Periventricular	0–2	0–2	0–4
Frontoparietal border area			
Subcortical	0–2	0–2	0–4
Periventricular	0–2	0–2	0–4
Parieto-occipital white matter			
Subcortical	0–2	0–2	0–4
Periventricular	0–2	0–2	0–4
Internal capsule			
ALIC	0–2	0–2	0–4
Pyramidal tracts in PLIC	0–2	0–2	0–4
Corpus callosum			
Genu	0–2	0–2	0–4
Splenium	0–2	0–2	0–4
Middle cerebellar peduncles ^a	0–2	0–2	0–4
Total white matter score	0–22	0–22	0–44
Atrophy score			
Supratentorial (bicaudate ratio)			0–2
Corpus callosum			0–2
Brainstem (pons diameter)			0–2
Cerebellar vermis			0–2
Cerebellar hemispheres			0–2
Atrophy score			0–10
Total score (white matter and atrophy)			0–54

Abbreviations: ALIC, anterior limb of the internal capsule; MRI, magnetic resonance imaging; PLIC, posterior limb of the internal capsule, T1W, T1-weighted; T2W, T2-weighted.

Notes: White matter scores, T1W images: 0 = hyperintense, 1 = isointense, 2 = hypointense in relation to caudate nucleus. T2W images: 0 = hypointense, 1 = isointense, 2 = hyperintense in relation to caudate nucleus.

Atrophy scores: bicaudate ratio and pons diameter (► **Tables 2** and **3**). Corpus callosum: 0 = normal, 1 = slightly thinned, 2 = severely thinned. Cerebellar vermis and cerebellar hemispheres: 0 = normal, 1 = mild atrophy with slightly enlarged interfolial spaces, 2 = severe atrophy with clearly enlarged interfolial spaces.

^aMiddle cerebellar peduncles: this item replaces cerebellar white matter in the original scoring system.

quantified using the BCR, defined as the smallest intercaudate distance divided by the transverse width of the inner table of the skull at the same level. These distances were measured on T2-weighted axial images with the smallest intercaudate distance (► **Fig. 2C, D**). Brainstem atrophy was quantified by measuring maximal anteroposterior diameter at the level

of the midpons on sagittal images (► **Fig. 2E**). Overall, patients could receive a score between 0 and 44 for hypomyelination and between 0 and 10 for atrophy, adding up to a total score of 0 to 54, with higher scores corresponding to more severe abnormalities.

Two neuroradiologists (F. B. and I. H.) and three pediatric neurologists (R. L. P., A. V., and G. B.), experienced in WM diseases, were asked to individually complete the scoring system for all patients. They were blinded to patient identifiers including age (the scores for the two age-dependent items, BCR and pons diameter, were deduced from the measurements the scorers provided). When three or more raters agreed on a score, this score was used for further analysis on clinical validity. Items for which less than three raters agreed on a score were sent for a second round of scoring to reach consensus. IRR was assessed for all individual MRI scoring items and measurements, as well as overall MRI severity scores, separately for the first and second rounds. Total MRI severity, hypomyelination, and atrophy scores were analyzed, including their association to factors such as age, gender, and mutated gene. For both pons diameter and BCR, age-related reference ranges were determined using scans of controls with normal MRI.

Correlation to Gross Motor Function

Patients were retrospectively classified according to the GMF classification system (GMFCS)¹⁷ based on clinical examination or clinical notes from the year in which the MRI study was performed. Retrospective estimation of GMF scores was previously shown to be reliable.¹⁸

Statistical Analysis

Data were analyzed by SPSS, version 20.0 for Windows (SPSS Inc., Chicago, IL), GraphPad Prism 7 (GraphPad Software, San Diego, CA), and R Software (R Foundation for statistical computing, Vienna, Austria). For determining reference ranges, normal values of BCR and pons diameter were plotted and, where appropriate, modeled by a (monotone) exponential curve fitted by means of nonlinear least squares. Subsequently, reference ranges were determined using population means and standard errors.

IRR was expressed using the single measure intraclass correlation coefficient (ICC), which was analyzed by means of a two-way mixed model based on absolute agreement (for separate items) or consistency (for total scores). Cutoffs for ICC were derived from Cicchetti, with ICC values less than 0.40 being considered as poor, values between 0.40 and 0.59 as fair, values between 0.60 and 0.74 as good, and values between 0.75 and 1.00 as excellent.¹⁹

Pearson (r) and Spearman (ρ) correlations were computed to determine associations between age, GMF, and MRI variables including total MRI score, hypomyelination, and atrophy scores. Subgroup differences for gender, gene mutation, and age groups were tested using a general linear model, analysis of variance, and Mann–Whitney U test and associated p -values. P -values of 0.05 or less were considered significant.

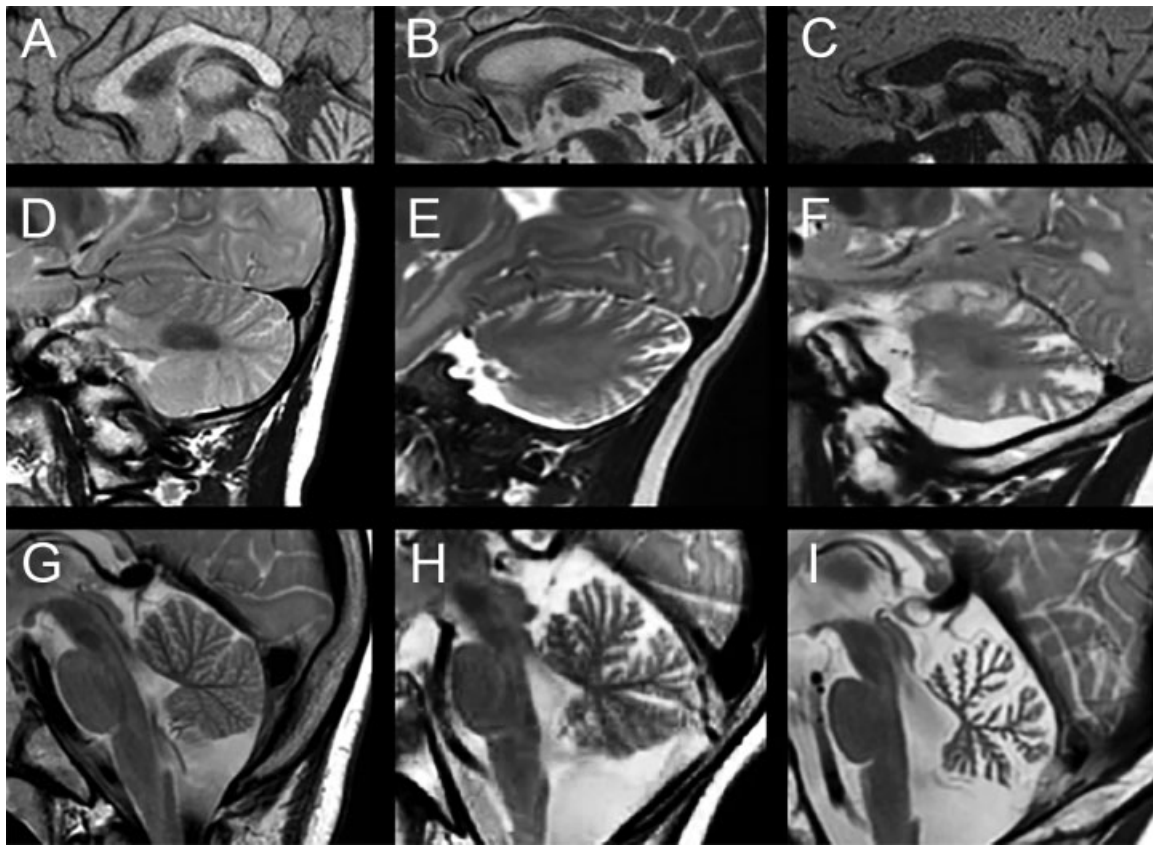


Fig. 1 Corpus callosum and cerebellar atrophy. (A) shows a normal corpus callosum with a score of 0 points, (B) shows a slightly thinned corpus callosum (score 1 point), and (C) shows a severely thinned corpus callosum (score 2 points). (D) depicts a normal cerebellar hemisphere (0 points), (E) depicts a mildly atrophic cerebellar hemisphere (1 point), and (F) depicts a severely atrophic cerebellar hemisphere (2 points). (G) displays a normal cerebellar vermis (0 points), (H) displays a mildly atrophic one (1 point), and (I) displays a severely atrophic cerebellar vermis (2 points).

Results

Patients and Controls

A total of 40 MRI brain scans (32 on a 1.5T scanner, 8 on a 3T scanner) were collected from 36 (19 females, 17 males) patients with genetically proven 4H with a median age of 12 years (range: 2–39 years). Six patients (four females, two males) had mutations in *POLR3A*, the majority, 27, in *POLR3B* (13 females, 14 males), and 3 in *POLR1C* (2 females, 1 male). Severity of clinical disease varied widely with GMFCS scores ranging from I ($n = 7$) to V ($n = 2$).

► **Fig. 2** shows the evolution of BCR and pons diameter in controls and patients. There was no significant difference between males and females. For grading brainstem and supratentorial atrophy in 4H, we pragmatically designed age groups using normal values (► **Fig. 2**; ► **Tables 2 and 3**).

In 4H patients, pons diameter was significantly smaller with a mean diameter of 18.38 mm (standard deviation [SD]: 1.98 mm) versus 20.86 mm (SD: 1.89 mm) in controls ($p < 0.01$). Similarly, BCR was found to be higher in patients with a mean BCR of 0.094 (SD: 0.026) versus 0.071 (SD: 0.015) in controls ($p < 0.01$). Although this difference was already present in younger patients, it further increased with age, indicating progressive volume loss.

Scoring Disagreement and Interrater Reliability

In the first round, a total of 1,080 scores were collected (27 items scored for 40 MRI scans). For only 48 (4.4%) scores, less than three raters agreed. In one single patient, the maximum number of items with disagreement was 3. After the second assessment of the 48 items with diverging scores, only 3 (0.3%) from the total of 1,080 scores remained without

Table 2 Scoring brainstem atrophy based on pons diameter

Score	2–3 y	4–5 y	6–7 y	8–9 y	10–12 y	13–14 y	15–19 y	20–22 y	≥ 23 y
0	≥18	≥19	≥19	≥20	≥20	≥21	≥21	≥22	≥22
1	17.99–16.01	18.99–16.01	18.99–17.01	19.99–17.01	19.99–18.01	20.99–18.01	20.99–19.01	21.99–19.01	21.99–20.01
2	≤16	≤16	≤17	≤17	≤18	≤18	≤19	≤19	≤20
Pons diameter (mm)									

Table 3 Scoring supratentorial atrophy based on bicaudate ratio

Score	2–9 y	10–18 y	19–23 y	≥ 24 y
0	<0.085	<0.090	<0.095	<0.100
1	0.085–0.100	0.090–0.105	0.095–0.110	0.100–0.115
2	>0.100	>0.105	>0.110	>0.115
	BCR			

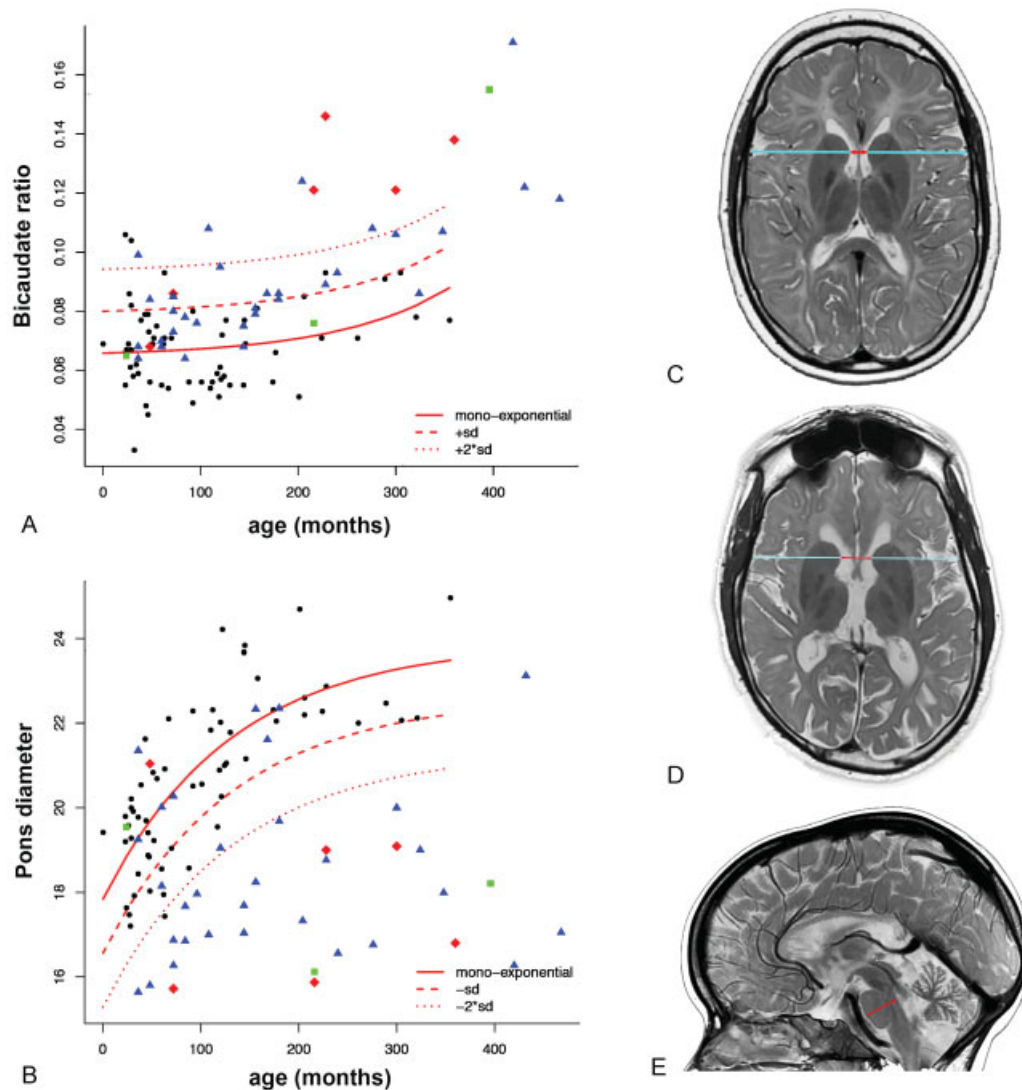


Fig. 2 Bicaudate ratio (BCR) and pons diameter in controls and patients. (A) Controls (black dots) with the (monotone) exponential curve (red) fitting best for this parameter (BCR = $b_0 + b_1 \cdot \exp(-\text{month}/t)$, with $b_0 = 0.00647$, $b_1 = 0.00105$, and $t = -114.9$; striped line, -1 standard deviation; dotted line, -2 standard deviations) and patients. Mainly, patients >16 years of age show supratentorial volume loss. (B) Evolution of pons diameter in controls (black dots), again with the (monotone) exponential curve (red) fitting best for this parameter (pons diameter = $b_0 + b_1 \cdot \exp(-\text{month}/t)$, with $b_0 = 23.90$, $b_1 = -6.06$, and $t = 132.6$; striped line, -1 standard deviation; dotted line, -2 standard deviations), and patients, showing early brainstem atrophy in 4H leukodystrophy patients. (C,D) Examples of measuring BCR in two patients, one with a normal result of 0.079 at age 13 years (C) and one with clear atrophy and a BCR of 0.155 at age 33 years (D). (E) Sagittal T2-weighted image of a young patient with normal pons diameter of 19.5 mm at the age of 2 years. Red diamonds, patients with mutations in *POLR3A*; blue triangles, patients with mutations in *POLR3B*; green squares, patients with mutations in *POLR1C*.

agreement of at least three raters. We refrained from imposing a consensus score and accepted that no consensus could be reached for these three items.

In the first round, IRR was found to be excellent for all subscores, with ICC values for consistency of 0.84 (95% confidence interval [CI]: 0.76–0.90) for hypomyelination, 0.88 (95% CI: 0.82–0.93) for atrophy, and 0.87 (95% CI: 0.80–0.92) for total MRI score. Overall, IRR was lower for items scored on T1-weighted scans, with some items showing a poor IRR (ICC < 0.40). These items included the periventricular frontoparietal border area, parieto-occipital WM (both subcortical and periventricular), the anterior limb of the internal capsule, and the cerebellar WM. In contrast, all items scored on T2-weighted images showed at least a fair IRR (ICC > 0.40). There was little disagreement on atrophy scores including those scores derived from pons diameter and BCR.

In the second round including the 48 scores with disagreement, results were largely similar. One of the difficult items to score was myelination of the cerebellar WM, especially in patients with severe cerebellar atrophy. We therefore considered omitting this region from the final score. Analyzing results without this item did not influence overall

outcome (not shown), and therefore we decided not to omit it from the scoring, but, to facilitate future use, to slightly modify the system by rating WM signal of the middle cerebellar peduncles instead.

MRI Severity, Hypomyelination, and Atrophy Scores

Median scores were 31/54 (range: 8–45) for total MRI score, 23/44 (range: 7–39) for hypomyelination, and 7/10 (range: 0–10) for atrophy. Scores tended to be higher in females than in males (median 34 vs. 26, respectively, $p = 0.024$). Total MRI scores did not significantly increase with age (►Fig. 3A). When looking at hypomyelination and atrophy scores separately, only atrophy scores were significantly correlated with age (►Fig. 3B, C). Global MRI and hypomyelination scores were significantly higher for patients with mutations in *POLR3A* than for patients with mutations in *POLR3B*, whereas atrophy scores were in the same range (►Fig. 4).

Magnetic Resonance Imaging Scores and Motor Disability

Patients with more limitations in GMF were found to have higher total MRI scores (►Fig. 3D). However, a large variability of MRI scores was seen with all GMFCS levels,

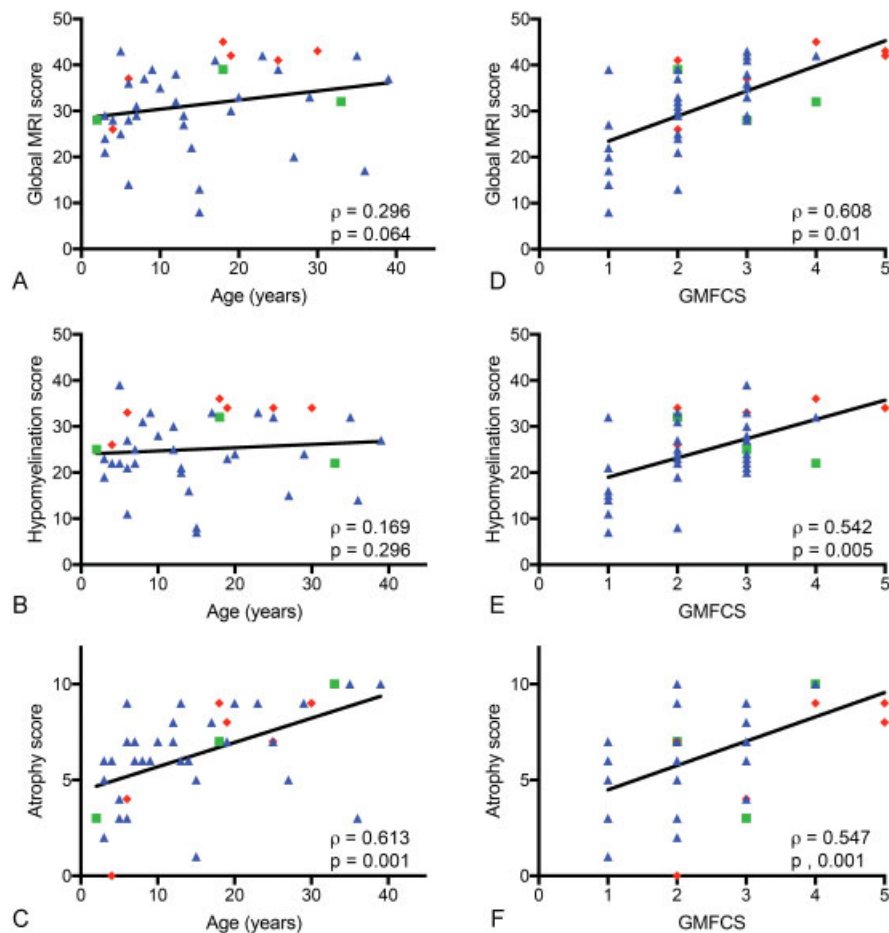


Fig. 3 Magnetic resonance imaging (MRI) scores in relation to age and gross motor function. Global MRI score (A) and hypomyelination score (B) do not show significant correlation with age, whereas atrophy is significantly correlated with age (C). All three scores significantly correlate with gross motor function (D–F). Red diamonds, patients with mutations in *POLR3A*; blue triangles, patients with mutations in *POLR3B*; green squares, patients with mutations in *POLR1C*.

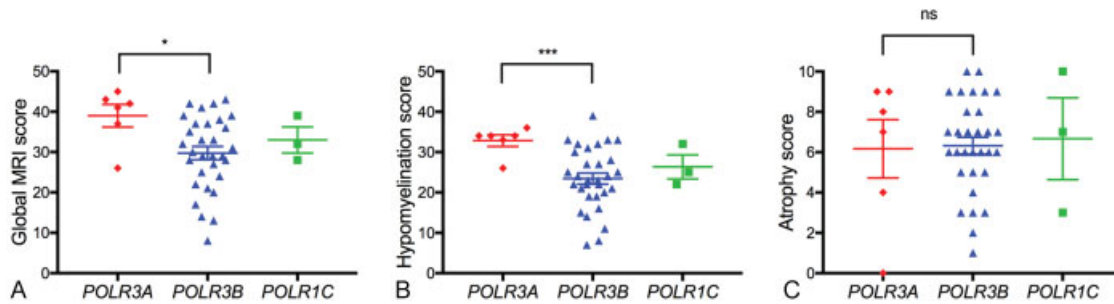


Fig. 4 Magnetic resonance imaging scores in relation to mutated gene. Score results (mean and standard error of the mean) depicted for the three patient groups (patients with mutations in *POLR3A*, *POLR3B* and *POLR1C*, respectively). Global (A) and hypomyelination (B) scores significantly differ between patients with *POLR3A* and *POLR3B* mutations (Mann–Whitney U test; * $p < 0.05$; *** $p < 0.001$). Atrophy scores do not show significant differences (C). We did not include the three patients with *POLR1C* mutations in this analysis as this latter group was very small. Diamonds, patients with mutations in *POLR3A*; triangles, patients with mutations in *POLR3B*; squares, patients with mutations in *POLR1C*.

interestingly most pronounced in patients with mild disability. A similar distribution was seen for hypomyelination and atrophy scores when analyzed separately, with increasing scores for more advanced clinical disease (► Fig. 3E, F).

Magnetic Resonance Imaging Scores at Follow-Up

Follow-up MRI examinations were available for four patients with a time interval ranging from 1 to 8 years between scans. Atrophy scores either remained stable ($n = 1$) or slightly worsened ($n = 3$). Hypomyelination scores, and therefore total MRI severity scores, improved in three of them. In those patients who showed improvement of hypomyelination scores, GMFCS remained stable ($n = 2$) or worsened slightly ($n = 1$).

Discussion

The aim of this study was to develop and validate a MRI scoring system for 4H, assessing hypomyelination and atrophy in this hypomyelinating disease. We decided to score both hypomyelination and atrophy, as cerebellar atrophy is a known early feature of 4H and as supratentorial atrophy slowly progresses with age. The authors of the recently published score for PMD independently also combined atrophy and myelination scores. They included fluid-attenuated inversion recovery (FLAIR) in addition to T1- and T2-weighted images, but omitted measurements to quantify atrophy.⁵

IRR was found to be excellent for hypomyelination, atrophy, and global MRI severity scores when assessed using ICC statistics. Nevertheless, in the first round, IRR varied between different items of the scoring system, with some items showing poor IRR, particularly those scored on T1-weighted images. Apparently, these items were more difficult to score or more sensitive to rater subjectivity. More precise instructions provided to the raters in the second round resulted in better agreement. As some atrophy items were assessed quantitatively (BCR,²⁰ pons diameter²¹), scoring of atrophy may be more objective than in the established scores for X-ALD or MLD.^{3,4} BCR was first described as a measure of atrophy in the 1980s and used for a variety of diseases including multiple sclerosis and Alzheimer's dis-

ease.^{22,23} Recently, one group used this parameter to measure brain atrophy in PMD.²⁴ In our patients, brainstem atrophy sets in much earlier than supratentorial atrophy, possibly at least in part due to the early cerebellar atrophy.

All MRI severity scores—hypomyelination, atrophy, and global scores—correlated with GMF, supporting the hypothesis that not only degree of hypomyelination but also atrophy codetermines handicap. A recent study on MRI changes in PMD reached similar conclusions, albeit less pronounced for myelination than for atrophy.⁵ Also in PMD, another group reported correlation of brain atrophy with disability, though without assessing myelination.²⁴ In multiple sclerosis, the prototype of acquired WM disease, brain atrophy is at least as important for clinical, especially cognitive impairment as WM lesions.^{25,26} Atrophy, in contrast to hypomyelination scores, clearly increased with age, suggesting age-dependent neuroaxonal loss rather than loss of myelin, although more long-term observations are needed to confirm this finding in larger patient groups. Interestingly, in 4H patients with mild clinical disease, MRI scores differed more widely than in patients with more severe disease, confirming our clinical experience.

In female patients, MRI scores tended to be higher than in male patients; this might be at least in part due to the fact that females were overrepresented in the group of patients with mutations in *POLR3A*. That in the four patients with follow-up scans there were some changes including improved myelination scores despite stable or slightly deteriorated GMFCS is difficult to interpret due to the small number of follow-up MRIs. Larger studies are needed to study evolution of MRI changes and clinical symptoms over time.

We recently described several patients with atypical forms of 4H, without clear myelin deficit and variable neurologic signs and symptoms.²⁷ Those patients were not included in this study as we focused on typical patients with hypomyelination, but it will be interesting to know whether significantly more myelin in these atypical cases also means less clinical handicap once enough cases will become available.

We were also interested in possible differences between patients with mutations in different genes. Although our

group consisted mainly of patients with mutations in *POLR3B*, patients with mutated *POLR3A* had higher mean MRI severity scores than the other two groups, consistent with the greater clinical severity with *POLR3A* mutations shown in our study on a large number of patients with 4H.¹⁵

One might wonder why, in the times of quantitative imaging and volumetry, we chose a comparably simple approach for this scoring system. It has several benefits: the sequences we used are part of standard protocols and therefore usually available, they can be compared among diverse scanners (with their slightly different protocols), and there is no need for specific control groups. Quantitative methods are more objective than a rater-dependent approach and often depend on specific scanners, making it laborious or even impossible to compare results between different centers or with changing MRI systems in even the same center. A robust, simple method as ours may be used in multicenter studies and also can make use of MRIs collected during a longer period, essential for a rare disease as 4H. These advantages are at the same time the limitations of this study: the use of different scanners with different field strengths and protocols and the retrospective setup may have affected results. That we did find correlations between MRI changes and clinical severity despite these odds, and that these correlations are comparable to other recent MRI studies on PMD, is encouraging and strengthens our interpretation.

In conclusion, this study shows that the proposed MRI scoring system reliably quantifies hypomyelination and atrophy, both correlating with clinical disease severity, in patients with 4H. It is easy to apply, even retrospectively, might serve as a useful biomarker for future studies, and can be used, with small adaptations, for other hypomyelinating disorders.

Funding

G. B. has received a Research Scholar Junior 1 award from the Fonds de Recherche du Québec en Santé 2012–2016 and a Canadian Institute of Health Research New Investigator salary award (2017–2022) (201512MSH-360766–171036). G. B. is also supported by a Canadian Institutes for Health Research grant (CIHR MOP-G-287547 and MOP-G2-341146–159133-BRIDG). F. K. C. is a recipient of the Directorate of Higher Education Overseas Scholarship–Dikti Scholarship, Ministry of National Education, Republic of Indonesia. F. B. is supported by the National Institute for Health Research Biomedical Research Centre at University College London Hospitals.

Acknowledgments

We thank all colleagues referring patients with 4H.

References

- Pouwels PJ, Vanderver A, Bernard G, et al. Hypomyelinating leukodystrophies: translational research progress and prospects. *Ann Neurol* 2014;76(1):5–19
- Steenweg ME, Wolf NI, van Wieringen WN, Barkhof F, van der Knaap MS, Pouwels PJ. Quantitative MRI in hypomyelinating disorders: correlation with motor handicap. *Neurology* 2016; 87(8):752–758
- Loes DJ, Hite S, Moser H, et al. Adrenoleukodystrophy: a scoring method for brain MR observations. *AJNR Am J Neuroradiol* 1994; 15(9):1761–1766
- Eichler F, Grodd W, Grant E, et al. Metachromatic leukodystrophy: a scoring system for brain MR imaging observations. *AJNR Am J Neuroradiol* 2009;30(10):1893–1897
- Sarret C, Lemaire JJ, Tonduti D, et al. Time-course of myelination and atrophy on cerebral imaging in 35 patients with PLP1-related disorders. *Dev Med Child Neurol* 2016;58(7):706–713
- Cayami FK, La Piana R, van Spaendonk RM, et al. *POLR3A* and *POLR3B* mutations in unclassified hypomyelination. *Neuropediatrics* 2015;46(3):221–228
- Wolf NI, Harting I, Boltshauser E, et al. Leukoencephalopathy with ataxia, hypodontia, and hypomyelination. *Neurology* 2005;64(8): 1461–1464
- Timmons M, Tsokos M, Asab MA, et al. Peripheral and central hypomyelination with hypogonadotropic hypogonadism and hypodontia. *Neurology* 2006;67(11):2066–2069
- Wolf NI, Harting I, Innes AM, et al. Ataxia, delayed dentition and hypomyelination: a novel leukoencephalopathy. *Neuropediatrics* 2007;38(2):64–70
- Bernard G, Chouery E, Putorti ML, et al. Mutations of *POLR3A* encoding a catalytic subunit of RNA polymerase Pol III cause a recessive hypomyelinating leukodystrophy. *Am J Hum Genet* 2011;89(3):415–423
- Saito H, Osaka H, Sasaki M, et al. Mutations in *POLR3A* and *POLR3B* encoding RNA Polymerase III subunits cause an autosomal-recessive hypomyelinating leukoencephalopathy. *Am J Hum Genet* 2011;89(5):644–651
- Daoud H, Tétéreault M, Gibson W, et al. Mutations in *POLR3A* and *POLR3B* are a major cause of hypomyelinating leukodystrophies with or without dental abnormalities and/or hypogonadotropic hypogonadism. *J Med Genet* 2013;50(3):194–197
- Thiffault I, Wolf NI, Forget D, et al. Recessive mutations in *POLR1C* cause a leukodystrophy by impairing biogenesis of RNA polymerase III. *Nat Commun* 2015;6:7623
- Tétéreault M, Choquet K, Orcesi S, et al. Recessive mutations in *POLR3B*, encoding the second largest subunit of Pol III, cause a rare hypomyelinating leukodystrophy. *Am J Hum Genet* 2011;89(5): 652–655
- Wolf NI, Vanderver A, van Spaendonk RM, et al. 4H Research Group. Clinical spectrum of 4H leukodystrophy caused by *POLR3A* and *POLR3B* mutations. *Neurology* 2014;83(21):1898–1905
- Steenweg ME, Vanderver A, Blaser S, et al. Magnetic resonance imaging pattern recognition in hypomyelinating disorders. *Brain* 2010;133(10):2971–2982
- Palisano R, Rosenbaum P, Walter S, Russell D, Wood E, Galuppi B. Development and reliability of a system to classify gross motor function in children with cerebral palsy. *Dev Med Child Neurol* 1997;39(4):214–223
- Mayson TA, Ward V, Davies KR, et al. Reliability of retrospective assignment of gross motor function classification system scores. *Dev Neurorehabil* 2013;16(3):207–209
- Cicchetti DV. Multiple comparison methods: establishing guidelines for their valid application in neuropsychological research. *J Clin Exp Neuropsychol* 1994;16(1):155–161
- Butzkueven H, Kolbe SC, Jolley DJ, et al. Validation of linear cerebral atrophy markers in multiple sclerosis. *J Clin Neurosci* 2008;15(2):130–137
- Raininko R, Autti T, Vanhanen SL, Ylikoski A, Erkinjuntti T, Santavuori P. The normal brain stem from infancy to old age. A morphometric MRI study. *Neuroradiology* 1994;36(5): 364–368

- 22 Caon C, Zvartau-Hind M, Ching W, Lisak RP, Tselis AC, Khan OA. Intercaudate nucleus ratio as a linear measure of brain atrophy in multiple sclerosis. *Neurology* 2003;60(2):323–325
- 23 Brickman AM, Honig LS, Scarmeas N, et al. Measuring cerebral atrophy and white matter hyperintensity burden to predict the rate of cognitive decline in Alzheimer disease. *Arch Neurol* 2008;65(9):1202–1208
- 24 Laukka JJ, Stanley JA, Garbern JY, et al. Neuroradiologic correlates of clinical disability and progression in the X-linked leukodystrophy Pelizaeus-Merzbacher disease. *J Neurol Sci* 2013;335(1-2):75–81
- 25 Bermel RA, Bakshi R. The measurement and clinical relevance of brain atrophy in multiple sclerosis. *Lancet Neurol* 2006;5(2):158–170
- 26 Roosendaal SD, Bendfeldt K, Vrenken H, et al. Grey matter volume in a large cohort of MS patients: relation to MRI parameters and disability. *Mult Scler* 2011;17(9):1098–1106
- 27 La Piana R, Cayami FK, Tran LT, et al. Diffuse hypomyelination is not obligate for *POLR3*-related disorders. *Neurology* 2016;86(17):1622–1626